

Systematic design of flat band slow light in photonic crystal waveguides

Juntao Li^{1,2}, Thomas P. White^{1*}, Liam O'Faolain¹, Alvaro Gomez-Iglesias¹, and Thomas F. Krauss¹

¹School of Physics and Astronomy, University of St Andrews, St Andrews, Fife, KY16 9SS, UK

²State Key Laboratory of Optoelectronic Materials and Technologies, Sun Yat-sen University, Guangzhou 510275, China

*Corresponding author: tom.white@st-andrews.ac.uk

Abstract: We present a systematic procedure for designing “flat bands” of photonic crystal waveguides for slow light propagation. The procedure aims to maximize the group index - bandwidth product by changing the position of the first two rows of holes of W1 line defect photonic crystal waveguides. A nearly constant group index - bandwidth product is achieved for group indices of 30-90 and as an example, we experimentally demonstrate flat band slow light with nearly constant group indices of 32.5, 44 and 49 over 14 nm, 11 nm and 9.5 nm bandwidth around 1550 nm, respectively.

©2008 Optical Society of America

OCIS codes: (130.5296) Photonic crystal waveguides; (999.9999) Slow light; (260.2030) Dispersion

References and Links

1. R. W. Boyd, D. J. Gauthier, and A. L. Gaeta, “Applications of slow light in telecommunications,” *Opt. Photon. News* **17**, 19-23 (2006).
2. T. F. Krauss, “Slow light in photonic crystal waveguides,” *J. Phys. D.* **40**, 2666-2670 (2007).
3. Y. A. Vlasov, M. O'Boyle, H. F. Hamann, and S. J. McNab, “Active control of slow light on a chip with photonic crystal waveguides,” *Nature* **438**, 65-69 (2005).
4. M. Soljacic and J. D. Joannopoulos, “Enhancement of nonlinear effects using photonic crystals,” *Nat. Mater.* **3**, 211-219 (2004).
5. J. T. Li and J. Y. Zhou, “Nonlinear optical frequency conversion with stopped short light pulses,” *Opt. Express* **14**, 2811-2816 (2006).
6. S. Hughes, L. Ramunno, J. F. Young, and J. E. Sipe, “Extrinsic optical scattering loss in photonic crystal waveguides: role of fabrication disorder and photon group velocity,” *Phys. Rev. Lett.* **94**, 033903 (2005).
7. R. J. P. Engelen, Y. Sugimoto, Y. Watanabe, J. P. Korterik, N. Ikeda, V. Hulst, K. Asakawa, and L. Kuipers, “The effect of higher-order dispersion on slow light propagation in photonic crystal waveguides,” *Opt. Express* **14**, 1658-1672 (2006).
8. D. Mori, S. Kubo, H. Sasaki, and T. Baba, “Wideband and low dispersion slow light by chirped photonic crystal coupled waveguide,” *Opt. Lett.* **15**, 5264-5270 (2007).
9. A. Yu. Petrov and M. Eich, “Zero dispersion at small group velocities in photonic crystal waveguides,” *Appl. Phys. Lett.* **85**, 4866-4868 (2004).
10. M. D. Settle, R. J. P. Engelen, M. Salib, A. Michaeli, L. Kuipers, and T. F. Krauss, “Flatband slow light in photonic crystals featuring spatial pulse compression and terahertz bandwidth,” *Opt. Express* **15**, 219-226 (2007).
11. J. M. Brosi, J. Leuthold, and W. Freude, “Microwave-frequency experiments validate optical simulation tools and demonstrate novel dispersion-tailored photonic crystal waveguides,” *J. Lightwave Technol.* **25**, 2502-2510 (2007).
12. L. H. Frandsen, A. V. Lavrinenko, J. Fage-Pedersen, and P. I. Borel, “Photonic crystal waveguides with semi-slow light and tailored dispersion properties,” *Opt. Express* **14**, 9444-9450 (2006).
13. S. Kubo, D. Mori, and T. Baba, “Low-group-velocity and low-dispersion slow light in photonic crystal waveguides,” *Opt. Lett.* **32**, 2981-2983 (2007).
14. M. Notomi, K. Yamada, A. Shinya, J. Takahashi, C. Takahashi, and I. Yokohama, “Extremely large group-velocity dispersion of line-defect waveguides in photonic crystal slabs,” *Phys. Rev. Lett.* **87**, 253902 (2001).
15. S. G. Johnson and J. D. Joannopoulos, “Block-iterative frequency-domain methods for Maxwell's equations in a planewave basis,” *Opt. Express* **8**, 173-190 (2001).
16. K. L. Lee, J. Bucchignano, J. Gelorme, and R. Viswanathan, “Ultrasonic and dip resist development processes for 50 nm device fabrication,” *J. Vac. Sci. Technol. B*, **15**, 2621-2626 (1997).
17. See <http://www.nanophotonics.eu>.

18. L. O'Faolain, X. Yuan, D. McIntyre, S. Thoms, H. Chong, R. M. De La Rue, and T. F. Krauss, "Low-loss propagation in photonic crystal waveguides," *Electron. Lett.* **42**, 1454-1455 (2006).
19. J. P. Hugonin, P. Lalanne, T. P. White, and T. F. Krauss, "Coupling into slow-mode photonic crystal waveguides," *Opt. Lett.* **32**, 2638-2640 (2007).
20. A. Gomez-Iglesias, D. O'Brien, L. O'Faolain, A. Miller, and T. F. Krauss, "Direct measurement of the group index of photonic crystal waveguides via Fourier transform spectral interferometry," *Appl. Phys. Lett.* **90**, 261107 (2007).
21. L. O'Faolain, T. P. White, D. O'Brien, X. Yuan, M. D. Settle, and T. F. Krauss, "Dependence of extrinsic loss on group velocity in photonic crystal waveguides," *Opt. Express* **15**, 13129-13138 (2007).

1. Introduction

Slow light in photonic crystal (PhC) waveguides can be exploited for a broad range of applications, such as optical delay lines or buffers [1] and enhanced light-matter interaction, both in the linear and nonlinear [2-5] regime. Two of the key concerns are propagation loss and dispersion, as any benefit arising from slow light may be compromised by excessive loss or pulse broadening [2,3,6,7]. This paper focuses on reducing the unwanted dispersion by engineering the dispersion curve with the aim of achieving a constant group index over a broad wavelength range, which we refer to as "flat band slow light".

Previously, flat band slow light has been achieved by chirping the waveguide properties [8], by changing the waveguide width [9-11], or by changing the hole size of the first two rows of the W1 PhC waveguides [12,13]. Some of these methods lead to multimode operation, others are difficult to control. Here, we study the properties of a PhC waveguide as a function of the position of the first two rows of holes adjacent to the line defect. Using this approach, we show that a continuous range of group indices from 30 to more 90 can be obtained that exhibits the desired flat band behavior and the same group index – bandwidth product. By plotting a map of group index – bandwidth product against the design parameters, we obtain a systematic picture of the relevant waveguide properties. To demonstrate the method, we fabricated W1 type waveguides that exhibit nearly constant group indices of 32.5, 44 and 49 over 14 nm, 11 nm and 9.5 nm bandwidth, respectively.

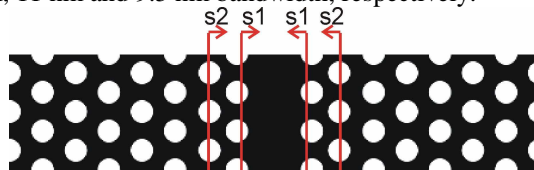


Fig. 1. Geometry of the modified W1 PhC waveguides: the first and second rows of holes are displaced symmetrically about the waveguide axis. The displacements relative to the unmodified lattice (red lines) are given by s_1 and s_2 , where shifts toward the waveguide centre are defined to be positive. Here, $s_1 < 0$ and $s_2 > 0$, as used throughout this paper.

2. Design

Line defect PhC waveguides support modes that can be categorized as either index guided or gap guided [14], or a combination of both. As explained in Refs. [9] and [14], an anti-crossing between these two types of modes determines the local shape of the waveguide mode dispersion curves, the slope of which determines the group velocity of the mode. Frandsen et al. [12] showed that changing the hole *size* of the first two rows of holes adjacent to the line defect waveguide can change the intrinsic interaction of the index guided and gap guided modes. Controlling this interaction can be used to modify the dispersion curve and thus to obtain a flat band slow light region. It is difficult however, to control the hole size of a photonic lattice accurately and reproducibly. Instead, we change here the *position* of the first two rows of holes in order to modify the dispersion curve – an approach that is technologically preferred to controlling variations in hole size. Figure 1 illustrates the displacement of the inner rows of holes that is used to modify the dispersion. Parameters s_1 and s_2 describe the deviation of each row from the ideal lattice.

To enable a comparison between waveguides, we define the figure of merit as the group index – bandwidth product, $n_g(\Delta\omega/\omega)$, which is proportional to the delay-bandwidth product per unit length. This value is then mapped as a function of parameters s_1 and s_2 as shown in Fig. 2. The group index n_g is considered as constant within a $\pm 10\%$ range, which is similar to previous work [10, 12]. In the calculation, the lattice constant was $a = 414$ nm, the normalised hole size $r/a = 0.286$, the thickness of the Si layer $h = 220$ nm and we considered TE polarisation. In Fig. 2(a), we used a two-dimensional (2D) version of the plane-wave expansion method [15] with an effective index of 2.87. The parameter scan was performed in steps of $s_1/a = 0.01$ ($s_1 = 4.14$ nm) and $s_2/a = 0.01$ ($s_2 = 4.14$ nm). For a more precise estimation, a three-dimensional (3D) calculation was used in the most promising range of s_1 and s_2 which is shown in Fig. 2(b) with steps of $s_1/a = 0.0025$ ($s_1 = 1.04$ nm) and $s_2/a = 0.005$ ($s_2 = 2.07$ nm). The result of 2D and 3D calculation is in good agreement, except that the group index and bandwidth are larger and narrower, respectively, for the 3D calculation. Different regimes of slow light operation can be recognized in the map.

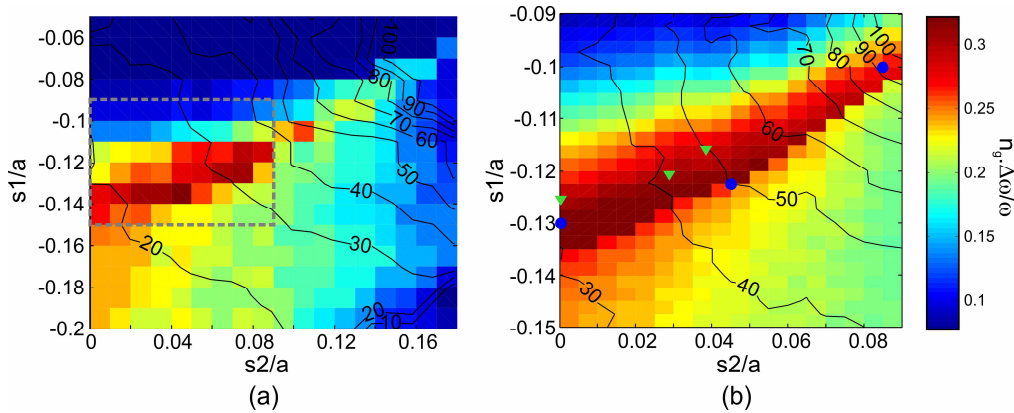


Fig. 2. Systematic maps of (a) 2D and (b) 3D calculations of the group index – bandwidth product as a function of s_1 and s_2 . The color plot and the contours represent $n_g(\Delta\omega/\omega)$ and n_g respectively. The rectangle in Fig. 2(a) indicates the calculation region of Fig. 2(b). The three blue circles and green triangles in Fig. 2(b) indicate the calculation points in Fig. 3 and the experimental points in Fig. 5 respectively.

In Fig. 2, the red region indicates high $n_g(\Delta\omega/\omega)$ values. The figure allows us to trace a flat band slow light region with an almost constant $n_g(\Delta\omega/\omega)$ value of approximately 0.3 but where the group index varies between $n_g = 30$ and $n_g = 90$. For comparison, $n_g(\Delta\omega/\omega) \approx 0.01$ for an unmodified W1 waveguide. When the group index is relatively low, the slow light mode is well confined within the first row of holes of the waveguide. Hence moderately slow light (up to $n_g = 35$) can be achieved without changing s_2 . When the light becomes slower, however, the mode penetrates deeper into the cladding and s_2 becomes significant. Therefore, achieving higher n_g values requires both s_1 and s_2 to be varied. In the experimental realization, we changed s_1 and s_2 in 2 nm steps, which corresponds to changing s_1/a or s_2/a by approximately 0.005. These tolerances limit the flat band slow light regime with the same $n_g(\Delta\omega/\omega)$ value to a group index of around $n_g = 50$, i.e. higher group indices (up to 200) would require control of s_1, s_2 on a smaller scale.

Figure 3 illustrates three operating points taken from Fig. 2(b) to highlight the evolution of the dispersion curves and group indices with increasing group index, i.e. $n_g=32, 50$ and 93 . The fundamental mode of an unmodified W1 PhC waveguide is shown for comparison. Note that the optimized group index curves in Fig. 3(b) have local minima and maxima where the group velocity dispersion (GVD) is zero, while the third order dispersion (TOD) passes through zero between these points. Alternative designs with simultaneous zero GVD and TOD can also be chosen from Fig. 2 with a slight bandwidth penalty.

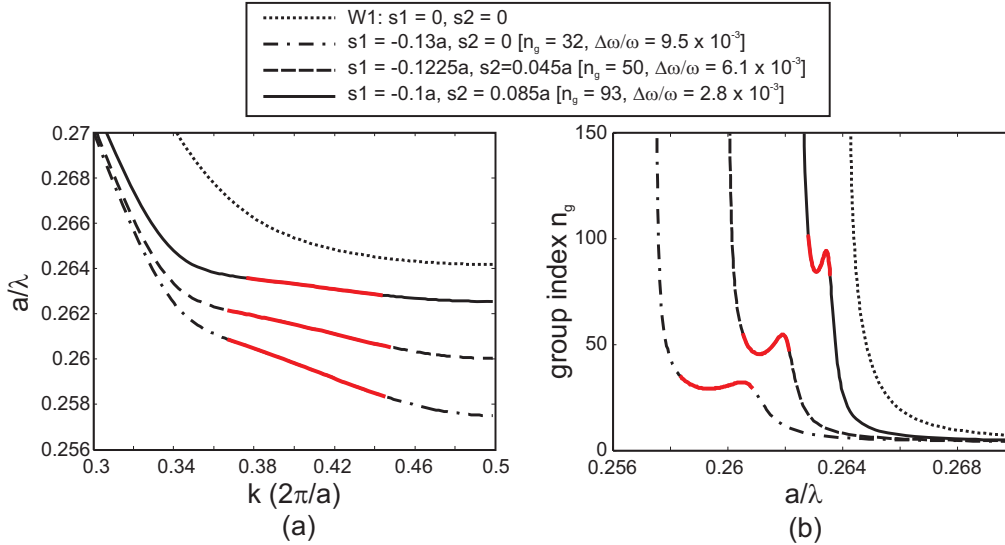


Fig. 3. (a) Calculated dispersion curves and (b) group indices, for the fundamental mode of the modified W1 PhC waveguides with $s1$ and $s2$ values indicated by the blue circles in Fig. 2(b). The thick solid red line represents the flat band slow light region. The group index – bandwidth product was around 0.3 in all cases. The result of W1 waveguide is also presented for comparison

There are some advantages of shifting rows of holes compared to changing the hole size [11]. First, variations in the hole position are easier to control technologically. Second, higher group indices (up to 200) can be achieved for a given group index - bandwidth product, especially if $s1, s2$ can be controlled more accurately than the 2 nm precision used here. In contrast, calculations show that it is difficult to achieve group indices higher than 100 by changing the hole size alone. Third, the maximum $n_g(\Delta\omega/\omega)$ in previous work [8,12,13] tended to decrease when the group index is increased, whereas we demonstrate that it is possible to change the group indices continuously while maintaining an almost constant maximum $n_g(\Delta\omega/\omega)$ by changing the hole positions according to Fig. 2.

3. Fabrication and experiment

The devices were fabricated on a SOITEC Silicon on Insulator wafer comprising a 220 nm thick Silicon layer on $2\mu\text{m}$ of silica. The pattern was exposed in ZEP520A electron beam resist using a hybrid ZEISS GEMINI 1530/RAITH ELPHY electron beam writer at 30keV with a pixel size of 2 nm and a writing field of $100\mu\text{m}$. The resist was developed using xylene with ultrasonic agitation [16]. Pattern transfer was carried out using Reactive Ion Etching with CHF_3 and SF_6 gases. The silica beneath the photonic crystal was removed using Hydrofluoric acid (the rest of the pattern was protected with photoresist)

The fabrication of these devices was carried out in the framework of the ePIXnet Nanostructuring Platform for Photonic Integration [17] and was very similar to that used in [18]. A propagation loss of 12 db/cm was measured for benchmark W1 waveguides. To enhance coupling into the slow light regime, an intermediate region consisting of ten periods of photonic crystal waveguide with a lattice constant of 444 nm was added at either end of the device, following the principles discussed in [19].

A typical SEM picture of our PhC waveguide design is shown in Fig. 4. $80\mu\text{m}$ long Si membrane W1 type PhC waveguides were made with a lattice constant $a = 414$ nm and hole diameter $d = 236$ nm ($r/a = 0.286$).

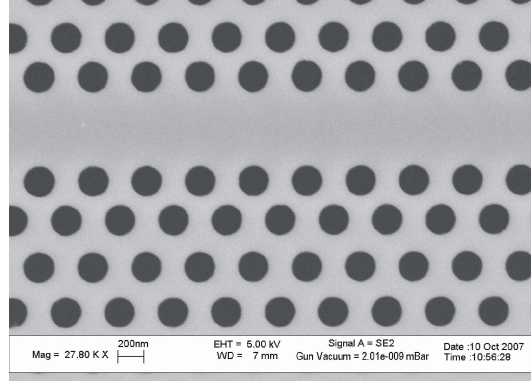


Fig. 4. Scanning electron micrograph (SEM) of a W1 type PhC waveguides with $s1 = -62$ nm and $s2 = 0$ nm.

Figure 2 shows that for any value of $s2$, we can find an $s1$ value to maximise $n_g(\Delta\omega/\omega)$. A range of group indices can be accessed in this way by choosing appropriate $s2$ values. Hence, to demonstrate our design, we fabricated and characterized three sets of PhC waveguides with $s2 = 0$ nm, 12 nm and 16 nm, and $s1$ values spanning the optimized region of Fig. 2(b) in 2 nm steps.

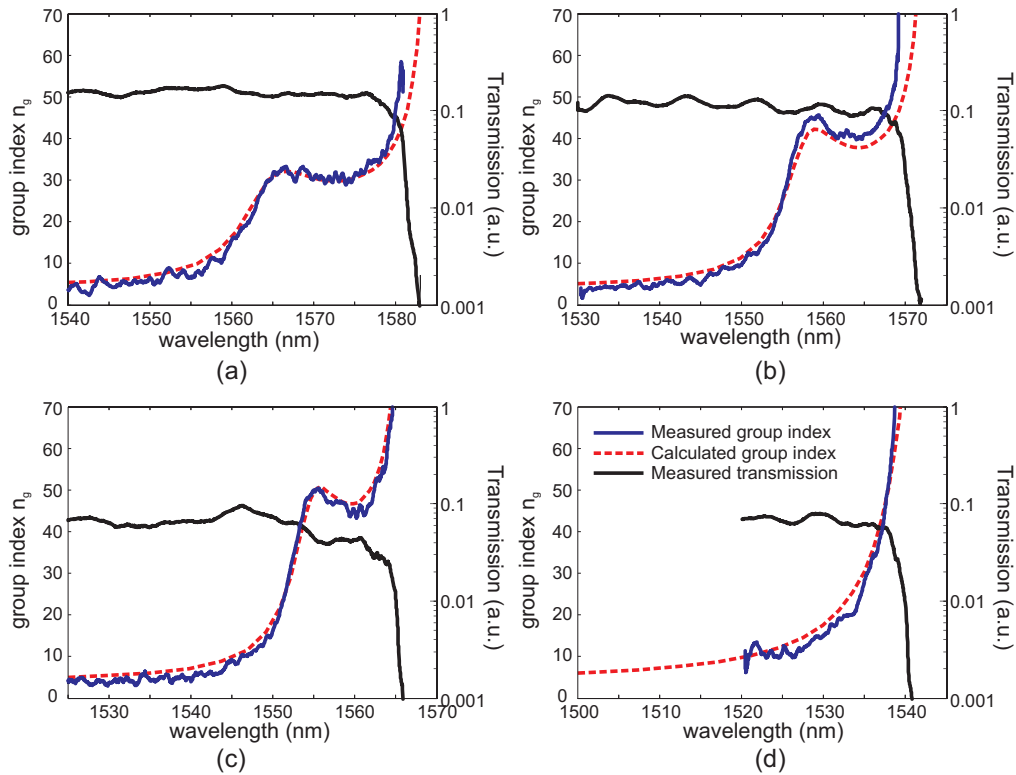


Fig. 5. Measured transmission spectra (black solid lines) and experiment (blue solid lines) and calculated (red dashed lines) group index of the PhC waveguides with $s1$ and $s2$ values indicated in Fig. 2(b): (a) $s1 = -52$ nm and $s2 = 0$ nm, (b) $s1 = -50$ nm and $s2 = 12$ nm, and (c) $s1 = -48$ nm and $s2 = 16$ nm. The flat band group index and the corresponding group index – bandwidth products are $n_g = 32.5$ for $n_g(\Delta\omega/\omega) = 0.29$, $n_g = 44$ for $n_g(\Delta\omega/\omega) = 0.31$, and $n_g = 49$ for $n_g(\Delta\omega/\omega) = 0.3$ respectively. The result of a normal W1 PhC waveguide is also presented for comparison (d).

Figure 5 shows the experimental transmission spectra and the experimental and calculated group indices for each value of s_2 and the corresponding s_1 that gave a maximum $n_g(\Delta\omega/\omega)$. The transmission was measured with a tuneable laser and the group indices were evaluated experimentally via Fourier transform spectral interferometry [20] using the same laser. The theoretical group index curves are calculated numerically via a 3D band structure calculation using the designed parameters [15]. The curves are red-shifted approximately 1.5% in wavelength to match the experiment results.

The change in group index with increasing s_2 is clearly illustrated in Fig. 5. The group indices are measured to be $n_g = 32.5$ (14 nm bandwidth), $n_g = 44$ (11.0 nm bandwidth) and $n_g = 49$ (9.5 nm bandwidth) resulting in a nearly constant group index – bandwidth product, which compares favourably with previous work [9-13]. The corresponding group velocity dispersion (calculated from the 3D simulation data) is one order of magnitude smaller than a W1 PhC waveguide at the same group index. Note also that the transmission spectra in Fig. 5(a) and (b) show no significant drop as the group index increases into the engineered slow light region, while in Fig. 5(c) the transmission decreases by only a factor of two for an almost ten-fold increase in group index. While additional measurements are required to quantify the propagation loss in the slow light region, these observations are consistent with our previous results for W1 waveguides [21] that show a much weaker dependence of losses on group velocity than initially assumed [6].

4. Conclusion

A systematic design for flat band slow light operation in PhC waveguides was carried out numerically; changing the position of the first two rows adjacent to the line defect waveguide gives access to a range of group indices, typically between $n_g = 30$ and 90, for an almost constant group index - bandwidth product. This approach has the technological advantage of holding the hole size constant across the device- it is generally observed during etching that features such as sidewall angle can vary with hole size (strongly so in our particular case). This effect may be small but is an important factor in minimizing propagation loss in slow light PhCs. Changing hole position may also be implemented with better control than changing the hole size, which is the method previously employed by others. Our method is experimentally demonstrated by three flat band slow light structures. These structures have a nearly constant group index - bandwidth product with group indices of 32.5, 44 and 49 over 14 nm, 11 nm and 9.5 nm bandwidth. Our new design approach shows the powerful possibilities of using PhC waveguides in the slow light regime for practical applications especially in the enhancement of linear and nonlinear effects.

Acknowledgments

This work was supported by the EU-FP6 “SPLASH” project and the International Program Fund of 985 Project of Sun Yat-Sen University. T.P. White is supported by an 1851 Royal Commission Research Fellowship, and the EU-FP6 Marie Curie Fellowship project “SLIPPRY”. L. O’Faolain is supported by the EU-FP6 Network of Excellence “ePIXnet”. The authors would like to acknowledge Maria Kotlyar, George Robb and Steve Balfour for help with the experiments and Dominik Szymanski for useful discussions.